ADVANCED MATERIALS
www.advmat.de

A Superhydrophobic Smart Coating for Flexible and Wearable Sensing Electronics

*Lianhui Li, Yuanyuan Bai, Lili Li, Shuqi Wang, and Ting Zhang**

Superhydrophobic surfaces have shown versatile applications in waterproofing, self-cleaning, drag reduction, selective absorption, etc. The most convenient and universally applicable approach to forming superhydrophobic surfaces is by coating; however, currently, superhydrophobic, smart coatings with flexibility and multiple functions for wearable sensing electronics are not yet reported. Here, a highly flexible multifunctional smart coating is fabricated by spray-coating multiwalled carbon nanotubes dispersed in a thermoplastic elastomer solution, followed by treatment with ethanol. The coatings not only endow various substrate materials with superhydrophobic surfaces, but can also respond to stretching, bending, and torsion—a property useful for flexible sensor applications. The coatings show superior sensitivity (gauge factor of 5.4–80), high resolution (1° of bending), a fast response time (<8 ms), a stable response over 5000 stretching–relaxing cycles, and wide sensing ranges (stretching: over 76%, bending: 0°–140°, torsion: 0–350 rad m^{-1}). Moreover, multifunctional coatings with thicknesses of only 1 μm can be directly applied to clothing for full-range and real-time detection of human motions, which also show extreme repellency to water, acid, and alkali, which helps the sensors to work under wet and corrosive conditions.

Superhydrophobic surfaces, generally characterized by a water contact angle (CA) over 150°, exist extensively in nature, for example the surface of lotus leaves[1,2] and water-strider legs.[3] Creating artificial superhydrophobic surfaces and exploring their versatile applications, such as waterproofing,[4] self-cleaning,[2,5] drag reduction,[6,7] and selective absorption,[8] have become exciting research frontiers. Tailoring the surface microtopography or surface free energy is usually required to endow a material surface with superhydrophobic properties,[9] for example, by applying an external force,[10] lithography,[11] mechanical assembly,[12] or chemical vapor deposition.[13] The most convenient and universally applicable approach to forming superhydrophobic surfaces is by coating.[4,5,14–16] Available coating materials reported in literature include porous polypropylene,[14] a commercial silicone sealant,[4] candle soot,[16] silicone nanofilaments,[15] and suspensions of perfluorosilane-coated titanium dioxide nanoparticles.[5] Generally, good stability, flexibility, practicability, and universality of superhydrophobic coatings are needed for practical use, and multifunctionality has been a new focus of superhydrophobic coatings. For example, superhydrophobic and conductive coatings[10,17] have been reported as promising conductors for electrode materials. Huang et al. reported lotus-leaf-like Cu-ferrite films with superhydrophobicity and magnetization.[18] Nonetheless, superhydrophobic smart coatings for wearable sensing applications have not yet been reported. Herein, we report a novel superhydrophobic and piezoresistive coating with high flexibility and universal applicability to various substrate materials. The coating films are fabricated by spray-coating of multiwalled carbon nanotubes (MWCNTs) dispersed in a thermoplastic elastomer (TPE) solution, followed by treatment with ethanol. The introduction of MWCNTs, with high intrinsic electrical conductivity, 1D, high aspect ratios, and excellent mechanical properties,[19] into the superelastic insulating TPE matrix not only induces micro-/nanostructured superhydrophobic surfaces, but also endows the composite coating with reversible elastic deformation and variable electrical sensing performance. The coatings show superior sensitivity (gauge factor (GF) of 5.4–80), high resolution (1° of bending), a fast response time (<8 ms), a stable response over 5000 stretching–relaxing cycles, and wide sensing ranges (stretching: over 76%, bending: 0°–140°, torsion: 0–350 rad m^{-1}). Moreover, the multifunctional smart coatings with thicknesses of only 1 μm could be directly applied to clothing as wearable sensors for full-range and real-time detection of human motions, which also show extreme repellency to water, acid, and alkali that help the sensors to work under wet and corrosive conditions.

MWCNTs were dispersed in cyclohexane by strong sonication, and the TPE elastomer was then dissolved through magnetic stirring and sonication to form a suspension. TPE acted as both the matrix and surfactant for the MWCNTs, so that the suspension had high stability with no MWCNT precipitation for at least three months (Figure S1, Supporting Information). The as-prepared suspension was coated onto a substrate via the spray-coating method, as illustrated in **Figure 1**a. The microstructured MWCNT/TPE coating film was gradually formed by controlling the spraying speed to balance the spraying and solvent evaporation time. It is important to maintain this balance

L. H. Li, Dr. Y. Y. Bai, L. L. Li, Dr. S. Q. Wang, Prof. T. Zhang
i-Lab, Suzhou Institute of Nano-Tech and Nano-Bionics (SINANO)
Chinese Academy of Sciences (CAS)
398 Ruoshui Road, Suzhou 215123, P. R. China
E-mail: tzhang2009@sinano.ac.cn

DOI: 10.1002/adma.201702517

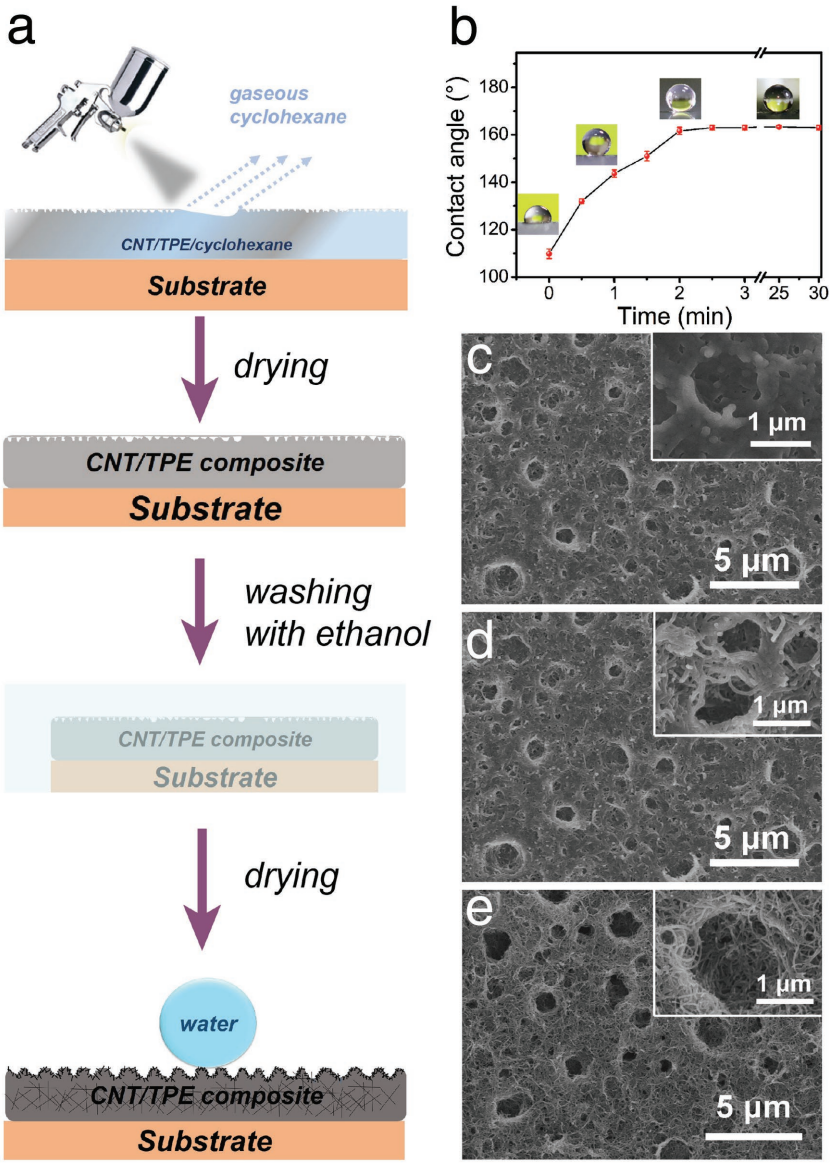

Figure 1. Preparation and SEM characterization of the MWCNT/TPE composite film coatings. a) Schematic illustration of the preparation procedure. b) Water contact angles on the coated substrates as a function of immersion time in ethanol. Insets: Representative optical photographs showing water droplets (≈3 µL) on the coated substrates. The error value was calculated as the standard deviation (S) of the measured CA values using the equation $S = \sqrt{\frac{1}{N-1}\sum_{i=1}^{N}(X_i - X)^2}$, where $N = 5$ is the number of measured water droplets on each MWCNT/TPE film, X_i is the CA value of water droplet i, and X is the average CA value of all measured water droplets. c–e) SEM images of the MWCNT/TPE-film surfaces after being treated in ethanol for 0 min (c), 1 min (d), 2 min (e). Insets: Enlarged images.

by properly controlling the airbrush pressure, moving speed of the spray-gun, and distance between the spray-gun and substrate. The water contact angle was measured (Figure S2, Supporting Information) to be 110°, verifying that the obtained film was hydrophobic. To enhance the water repellency, the film was immersed in absolute ethanol to treat its surface. Figure 1b shows the measured water contact angle as a function of the ethanol treatment time. As the time increased, CA gradually increased, and at 1.3 min, CA reached 150°, indicating the transformation of the film surface from hydrophobic to superhydrophobic. As the treatment time increased to 2 min, CA increased to 162°, and with a further increase of the time to 30 min, CA did not show apparent increase, reflecting that the film surface tended to reach a stable superhydrophobic state after being treated for over 2 min. A water dropping test was carried out on a piece of MWCNT/TPE film treated with ethanol for 2 min on a glass substrate with a tilt angle of ≈2.3° (Movie S1, Supporting Information). Water droplets rolled off almost immediately after being dropped on the film, indicating that the surface was extremely water repellent (or superhydrophobic) and that its critical sliding angle was smaller than 2.3°.

To explain the main mechanism underlying the transformation of water repellency of the MWCNT/TPE coating film, the surface microtopography of MWCNT/TPE films with different treatment times in ethanol was characterized by scanning electron microscopy (SEM), as shown in Figure 1c–e. For the MWCNT/TPE film not treated with ethanol (Figure 1c), most of the MWCNTs were encapsulated by TPE polymer. In addition, large amounts of micrometer-sized pit-like features existed on the film surface. These features mainly resulted from the following preparation method. When a cyclohexane suspension of MWCNTs and TPE was sprayed on a substrate, a solid–liquid MWCNT/TPE/cyclohexane film was initially formed. Then, impact forces from the continuous spraying of liquid droplets acted on the solid–liquid surface, thus generating large amounts of micrometer-sized features, which were then immobilized during the fast evaporation of cyclohexane. For the MWCNT/TPE film treated with ethanol for 1 min, absolute ethanol partially dissolved the TPE and introduced air gaps between MWCNTs (encapsulated by TPE), as shown in Figure 1d. With a longer treatment time of 2 min, more TPE were dissolved and the film surface formed a network with many pit-like features (Figure 1e). Figure S3 (Supporting Information) presents the surface microtopography of the film treated for 30 min, which does not show much difference with that treated for 2 min, implying that most of the TPE near the surface might have been dissolved within about 2 min. The atomic force microscope (AFM) was used to quantitatively evaluate the variation of the film surface roughness, and a typical 3D AFM image showing the surface height variation of a piece of as-prepared MWCNT/TPE composite film is given in Figure S4 (Supporting Information). The surface roughness

factor defined as the ratio between the actual surface area and the projected surface area[20] was obtained directly using the Nano Scope Analysis software, which was 1.17, 1.24, 1.26, 1.27 for the coating film treated with ethanol for 0 (as prepared), 1, 2, and 30 min, respectively. The relationship between the surface roughness and the water contact angles of the films is discussed as follows according to the Wenzel and Cassie models[9] described by Equation (1) and (2)

$$\cos\theta = r\cos\theta_0 \quad (\text{at Wenzel state}) \tag{1}$$

$$\cos\theta = -1 + (1 - f_a)(\cos\theta_0 + 1) \quad (\text{at Cassie state}) \tag{2}$$

where θ is the apparent contact angle of a water droplet on a rough film surface; r is the film surface roughness; f_a is the air fraction in the contact area in the Cassie state; θ_0 is the water contact angle of the ideal MWCNT/TPE film, which is smooth and homogeneous. As an approximation, we suppose that all MWCNTs are encapsulated by TPE before surface treatment; therefore, θ_0 is the water contact angle on the TPE film, which is measured to be 105°.

In the beginning, a water droplet on the MWCNT/TPE film is in the Wenzel state and the apparent contact angle θ will increase with the increase of the surface roughness r according to Equation (1). When it turns to the Cassie state, θ will increase with the increase of the air fraction f_a according to Equation (2). The above results derived from the SEM and AFM measurements show that r and f_a both increase with increasing ethanol-treatment time; therefore, the gradual transformation of the MWCNT/TPE film from hydrophobic to superhydrophobic with increasing treatment time in ethanol can be explained well. Note that when the treatment time is longer than 2 min, most of the TPE near the surface have been dissolved and the increment of r and f_a over time is quite small, so θ does not increase, which is in accordance with Figure 1b.

The durability and stability of the superhydrophobicity were investigated, owing to their importance in practical use. To test these parameters, a piece of cloth coated with MWCNT/TPE film treated with ethanol for 2 min was kneaded for 300 times and still showed extreme water repellency (**Figure 2**a–c and Movie S2 (Supporting Information)), indicating that the coating film had excellent mechanical flexibility, strong adhesion with the substrate, and highly stable superhydrophobic surface. To explain the superior mechanical performance, the cross-sectional micromorphology of the TPE was characterized by SEM. As shown in Figure 2d, despite that the TPE near the surface was dissolved by ethanol, the middle parts of the MWCNTs were still encapsulated by TPE and extended to the inner film to act as the tightly entangled "bridges" across the whole film. Moreover, in the bottom part of the film, MWCNTs were encapsulated by large amount of TPE, which helped the film to adhere tightly to the substrate. The superior elasticity of TPE endowed the networks with reversible elastic deformation, enabling the film to deform with the substrate without sliding or detaching. In contrast, the coating film treated with ethanol for 30 min showed severely deteriorated mechanical property and poor adhesion with the substrate (Figure S5, Supporting Information) due to the dissolution of the inner TPE. Therefore, an ethanol-treatment time of 2 min was adopted for the following experiments in this paper to ensure a great mechanical and superhydrophobic stability of the coating films. Outdoors, the superhydrophobicity of a surface may deteriorate after exposure to ultraviolet (UV) radiation from sunlight or acid/alkali stress from the surroundings. The influence of these factors on our superhydrophobic surface is presented in Figure 2e. Glass substrates coated with MWCNT/TPE films were exposed to UV radiation for 48 h using a portable UV analyzer (WFH-204B, Qiwei incorporation, China) at 256 nm (equivalent to a 15 d exposure in a natural environment) or immersed in a 1 mol L^{-1} HCl aqueous solution or NaOH aqueous solution for 12 h. The microtopography of the coating films did not show apparent difference according to their SEM images (Figure S6, Supporting Information) and the measured water contact angles decreased only slightly from 162° to 160°, 157°, and 158°, respectively, indicating the high stability of the surface superhydrophobicity. Additionally, some superhydrophobic surfaces are unstable under the long-term stress of water droplets; therefore, we further examined the water contact angle on the coated MWCNT/TPE film over 20 min (Figure S7, Supporting Information). No noticeable CA (≈160°) changes were observed over time, indicating that the surface superhydrophobicity had long-term stability. Figure S7 (Supporting Information) also shows the measured contact angles of acidic/alkaline aqueous droplets on MWCNT/TPE film. The CA values of the extreme acidic aqueous droplets were slightly smaller (pH of 0–5, CA of 155°–158°) than those of weakly acidic or alkaline aqueous droplets (pH of 6–14, CA of 159°–161°), which might be due to the difference in the chemical property and surface tension of the droplets with different pH. Nevertheless, the measured CA values were all larger than 150°, thus indicating the extreme repellency of the film to both acid and alkali solutions. The verified good durability and stability of the superhydrophobic MWCNT/TPE coating can be explained as follows. The TPE used in this work was a hydrogenated styrene–ethylene/butylene–styrene (SEBS) block copolymer, which has no unsaturated double bonds in its molecular structure and does not react with acid–bases. SEBS also has good stability to UV radiation.[21] Therefore, when exposed to the above-tested factors, TPE acts as a protective layer that keeps the microtopology of the coating intact and imparts high durability and stability. These experimental results suggested that the present coating has a superior ability to protect its substrate from being corroded by water, acid, or alkali in outdoor use.

We next investigated the feasibility of superhydrophobic MWCNT/TPE coatings in waterproofing and drag reduction applications. The MWCNT/TPE film was readily coated on a fabric glove, which was subsequently immersed in water. After removal from the water, the coated glove was completely dry (**Figure 3**a,b and Movie S3 (Supporting Information)), indicating an excellent waterproofing ability of the coating. For comparison, an uncoated glove was completely wet after the same process (Figure S8, Supporting Information). To examine the drag-reduction ability, magnetic MWCNT/Fe_3O_4/TPE films were coated on the four "feet" of a strider-like copper robot, which was subsequently placed on water. The coated robot easily "stood" on water and was driven freely by a magnet; in contrast, the uncoated robot could not "stand" on water

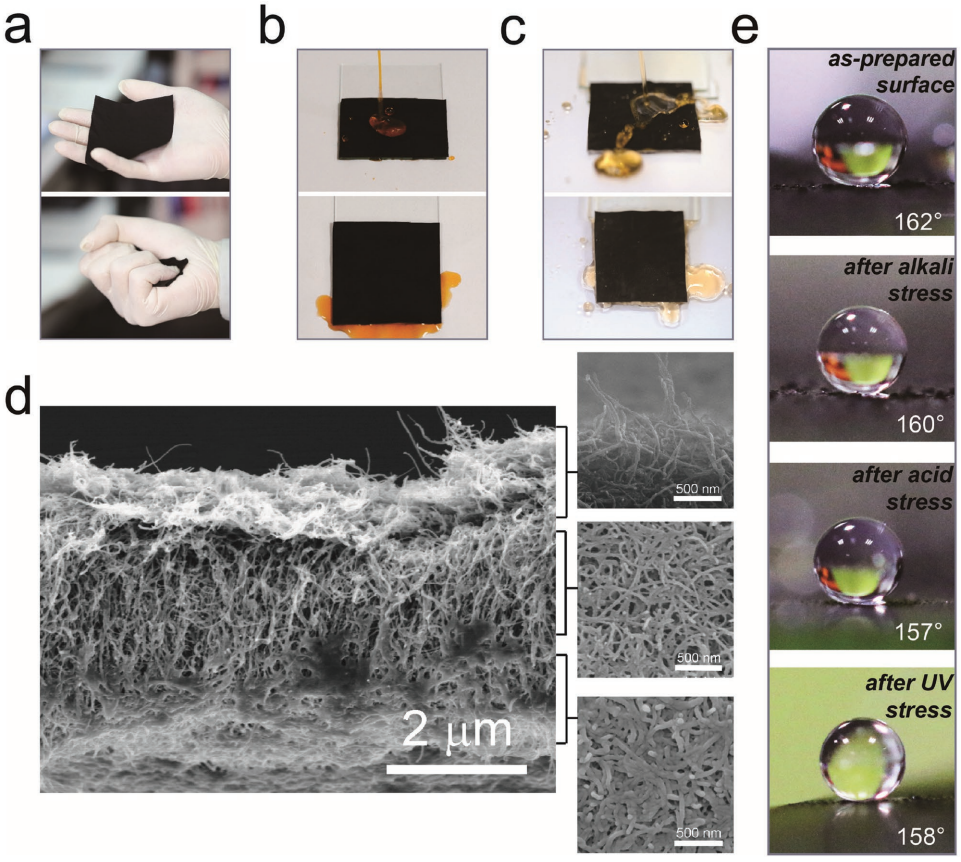

Figure 2. Superhydrophobic stability characterization of the MWCNT/TPE composite film coatings. a) Typical photographs showing the procedure of kneading a piece of coated cloth. b) Water repellency of coated cloth as-prepared. c) Water repellency of coated cloth after being kneaded for 300 times, showing the high superhydrophobic stability of MWCNT/TPE film on cloth. d) SEM image showing the cross-sectional micromorphology of MWCNT/TPE composite film treated with ethanol for 2 min. e) Optical photographs showing the contact angles of water droplets (≈3 μL) on coated glass substrates as-prepared and after different treatments.

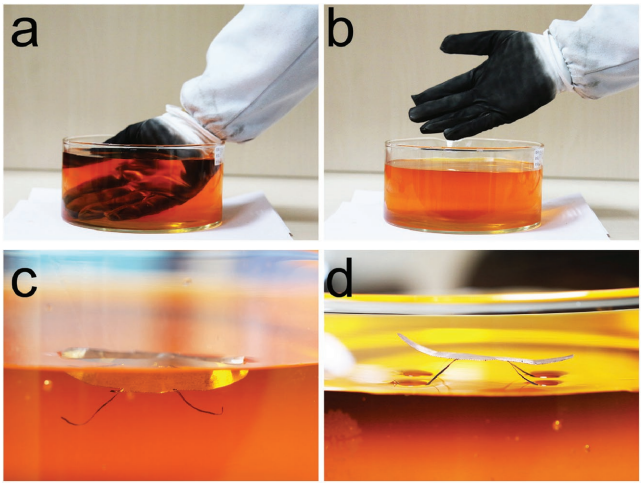

Figure 3. Applications of the superhydrophobic MWCNT/TPE-film coating for waterproofing and drag reduction. a,b) Representative optical photographs showing the procedure of dipping a coated fabric glove into water. c) Optical photograph of an uncoated strider-like copper robot on water. d) Optical photograph of a strider-like copper robot on water, with the four "feet" of the robot coated with magnetic MWCNT/Fe_3O_4/TPE films. In the experiments, colored pigment was added into the water for better observation.

(Figure 3c,d and Movie S4 (Supporting Information)). This phenomenon can be explained by the large amount of small air bubbles trapped between the superhydrophobic film surface and the water,[6] which enhanced the buoyancy on water, thus allowing the coated robot to "stand" on water. The air bubbles will also reduce the frictional drag when the robot is moving.

Apart from the superhydrophobic property of MWCNT/TPE coating discussed above, the introduction of conductive MWCNTs into the insulating TPE polymer also endows the composite coating with piezoresistive characteristics, since the MWCNTs form interconnected networks in the TPE matrix. When the composite film is tensile strained, the crosslinking degree of MWCNT networks decreases, which results in a smaller number of conductive paths for electrons and an increased film resistance. In contrast, when the composite film is compressed, its resistance decreases. Accordingly, we developed flexible strain sensors by using the superhydrophobic MWCNT/TPE coating film, and their sensing performance toward stretching, bending, and torsion were investigated in detail.

A MWCNT/TPE-film sensor on a strip of flexible silicone rubber (inset of **Figure 4**a) was gradually stretched to different tensile states. The tensile strain (ε) of the MWCNT/TPE film was calculated according to Equation (3):

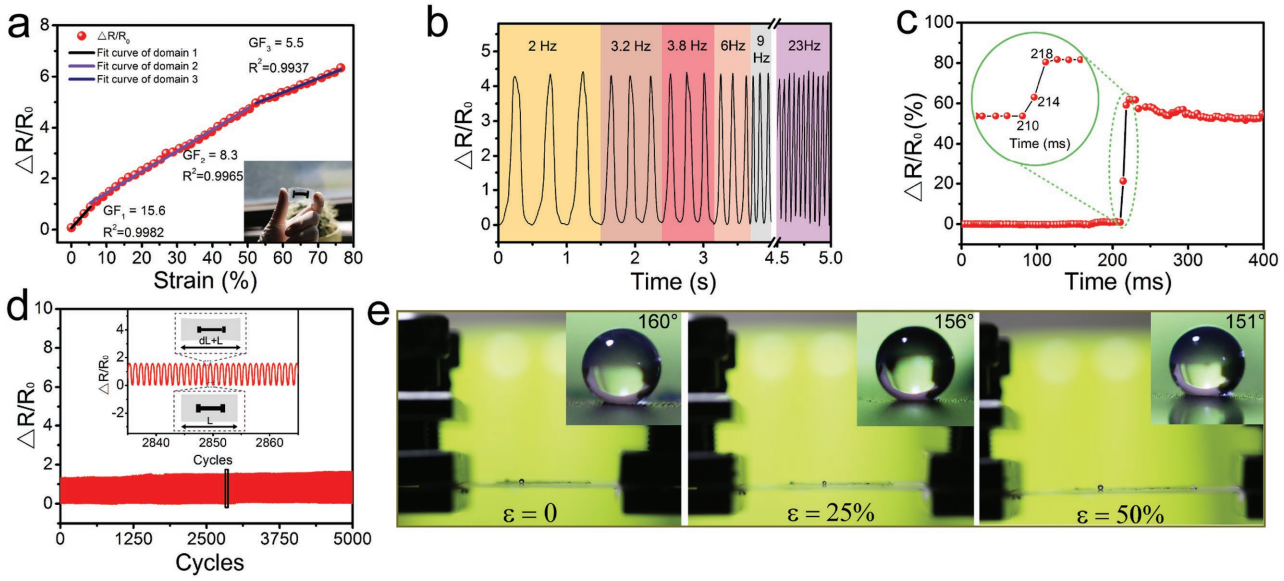

Figure 4. Sensing performance of the MWCNT/TPE-film sensor coated on a strip of silicone toward stretching and its surface water repellency investigations. a) Normalized relative resistance as a function of tensile strain and the linear fittings. Inset: Optical photograph of the sensor. b) Real-time variation in the resistance under repetitive stretching from $\varepsilon = 0\%$ to $\varepsilon = 50\%$ with different frequencies. c) Time response of the sensor upon applying a quasitransient step strain from $\varepsilon = 0\%$ to $\varepsilon = 5\%$. Inset: Enlarged figure showing the response time. d) Normalized relative resistance variation under cyclic stretching from $\varepsilon = 0\%$ to $\varepsilon = 10\%$ with a frequency of 0.5 Hz over 5000 cycles, which shows the reproducibility and durability of the sensor. e) Optical photographs of water droplets (≈3 μL) on the MWCNT/TPE film with different tensile strains. Insets: Enlarged photographs showing the water contact angles.

$$\varepsilon = (L - L_0)/L_0 \tag{3}$$

where L and L_0 are the film length at the tensile state and the relaxed state, respectively. The resistance (R) of the MWCNT/TPE film was measured in real time during stretching, and the normalized relative resistance ($\Delta R/R_0$) was calculated as

$$\Delta R/R_0 = (R - R_0)/R_0 \tag{4}$$

where R_0 is the film resistance at the relaxed state. $\Delta R/R_0$ as a function of ε is present in Figure 4a. $\Delta R/R_0$ increases monotonically with tensile strain up to ε = 76%, which is high enough for the film to be used as a wearable physical sensor in personal healthcare (primary sensing target: ε < 55%).[22] GFs, the representative parameters to access strain sensitivity, were calculated ($\Delta R/R_0/\varepsilon$) to be 15.6 (ε: < 6%), 8.1 (ε: 15–50%), and 5.4 (ε: 55–76%). The real-time variation in the resistance of the MWCNT/TPE-film sensor under repetitive stretching from ε = 0% to ε = 50% at different frequencies is shown in Figure 4b. The sensor exhibited a highly reproducible response, making it applicable to the detection of human activities with different frequencies, for example, blinking (0.1–0.5 Hz for healthy adults) or hand tremors of patients with parkinsonism (6–8 Hz). The response time of the sensor was measured by application of a quasitransient stretching to the substrate (Figure S9 and S10, Supporting Information). As shown in Figure 4c, the sensor exhibited a response time of only 8 ms, which was much faster than recently reported values of other strain sensors (70–110 ms).[23] Figure 4d presents the variation in the resistance of the sensor during cyclical stretching from ε = 0% to ε = 10% with a frequency of 0.5 Hz for 5000 cycles. $\Delta R/R_0$ varied periodically, and the maximum value of each cycle did not show an apparent change, thus indicating a high reproducibility and durability of the sensor. Furthermore, the water repellency and superhydrophobic stability of the surface during stretching are characterized in Figure 4e. As the MWCNT/TPE film was stretched, its water contact angle slightly decreased, owing to a decreased surface roughness of film under tensile strain. Nonetheless, the film remained superhydrophobic up to ε = 50% (160°/0% strain → 156°/25% strain → 151°/50% strain).

In addition to stretching, bending and torsion are also commonly observed in human activities, such as the bending and twisting of human joints. Therefore, we coated the MWCNT/TPE superhydrophobic film on a flexible silicone cylinder (**Figure 5**a) to measure its sensing performance during bending and torsion. When the substrate was bent inward, its outer surface, as well as the MWCNT/TPE-film coating, sustained tensile strain, which caused an increase in the film resistance. The film sensor exhibited a broad sensing range up to a bending angle of 140° (see Figure S11 in the Supporting Information for detailed bending angle measurement), with an accompanying large variation in the resistance of $\Delta R/R_0 > 3$ (Figure 5b), making the sensor suitable for detecting large-scale human motions (e.g., bending movements of the hands, arms, legs, and spine). For the detection of small bending angles, a detection resolution of 1° with a small induced tensile strain of 0.1%, calculated using Equation S1 (detailed information is given in Figure S12 in the Supporting Information), was achieved and is shown in Figure 5c,d. The GF values, calculated to be 19–80, were superior to those of previously reported highly stretchable composite sensors (GF: 0.5–69).[22,24,25] For the detection of

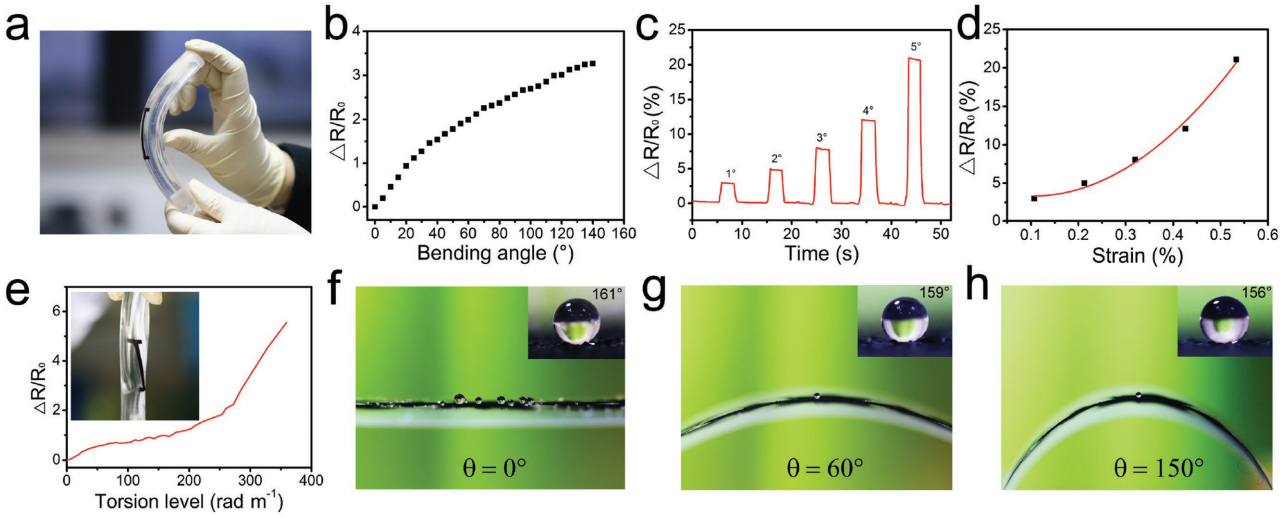

Figure 5. Sensing performance of the MWCNT/TPE-film sensor coated on a cylindrical silicone substrate toward bending/torsion and its surface water repellency investigations. a) Optical photograph of the sensor. b) Normalized relative resistance as a function of bending angle. c) Normalized relative resistance variation of the sensor after application of incremental bending steps from $\theta = 1°$ to $\theta = 5°$. d) Normalized relative resistance variation as a function of tensile strain induced by small bending angles. e) Normalized relative resistance as a function of torsion angle. Inset: Optical photograph of the sensor showing a typical torsion state. f–h) Optical photographs of water droplets (≈3 µL) on the coated film with different bending angles. Insets: Enlarged photographs showing the water contact angles.

torsional measurement, resistance of MWCNT/TPE sensor on a cylindrical silicone substrate was measured under the application of different levels of torsion along the clockwise direction (Figure 5e). A wide torsion sensing range of 0–350 rad m^{-1} was observed, with a large change in the normalized relative resistance ($\Delta R/R_0 > 5$). When the torsion level was higher than 350 rad m^{-1}, the cylindrical silicone substrate mechanically broke down, suggesting that the torsion sensing range of the MWCNT/TPE film can be expanded by use of substrates with better mechanical properties. For torsion along the anticlockwise direction, the response of the sensor would be the same as that along the clockwise direction, because the MWCNT/TPE film is fully isotropic. Then, variations in the surface water repellency of MWCNT/TPE film under bending were characterized, as shown in Figure 5f–h. Because of the difficulty in measuring the contact angles of water droplets on a cylindrical substrate, we coated the MWCNT/TPE film on a poly(ethylene terephthalate) (PET) plastic substrate instead (Figure S13, Supporting Information). As the MWCNT/TPE film was bended up to $\theta = 150$○, its water contact angle only decreased by 5° (from 161° to 156°), indicating that the film remained superhydrophobic over the entire achieved sensing range (0°–140°).

Finally, a useful practical application of the superhydrophobic smart MWCNT/TPE coating was demonstrated by fabricating wearable multifunctional sensors for the detection of human motions, which are widely used in personal healthcare[22,26] and human–machine interfaces.[25,27] A smart glove was readily achieved by coating with the multifunctional MWCNT/TPE films (**Figure 6**a). Figure 6b and Movie S5 (Supporting Information) present the real-time bending movement detection of an index finger wearing the smart glove. As the index finger was slowly and repeatedly bended and

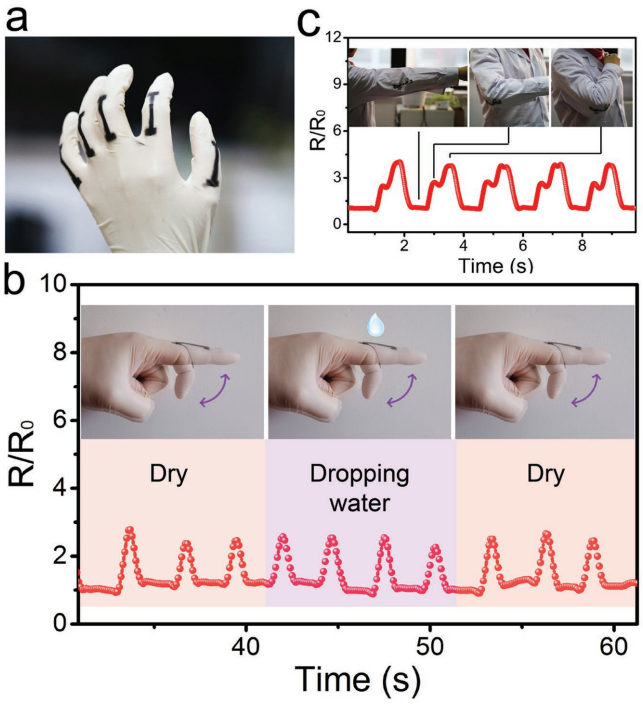

Figure 6. Real-time human motion detection using superhydrophobic MWCNT/TPE-film sensors. a) Optical photograph of a latex glove with five film sensors coated on each finger. b) Normalized relative resistance as a function of time. Insets: Schematics showing the repetitive bending of the index finger wearing a coated glove under discontinuous water dropping. c) Real-time variation of the normalized relative resistance. Insets: Optical photographs showing the bending movement of the elbow joint wearing coated lab gown.

relaxed, its normalized relative resistance showed a gradual and periodic synchronous increase and decrease, realizing the real-time detection of the index finger movement (the slight difference between each cycle resulted from the slight discrepancy of each bend). Moreover, the performance of the coated MWCNT/TPE-film sensor was not affected by intermittent water droplets, because the droplets rolled off the superhydrophobic surface almost immediately, thus indicating that the sensor can function under wet or rainy conditions. Similarly, the MWCNT/TPE smart coating was painted on a lab-gown sleeve and applied to real-time monitoring of elbow joint movement (Figure 6c). The bending degree of the elbow joint was reflected by the different maximum values of the relative resistance, with a larger maximum value corresponding to a higher bending angle. With more sophisticated architectural design, our stretchable smart sensors have the potential to detect additional physical signals for human healthcare and other applications.

In summary, a superhydrophobic MWCNT/TPE smart coating with high-performance sensing ability toward stretching, bending, and torsion was developed, which can be easily fabricated under ambient conditions with no special requirements for cleaning or activation of the substrate. The superhydrophobicity of the as-prepared MWCNT/TPE coating can endow various common objects (e.g., glass, plastic, cloth, and metals) with superhydrophobic properties for self-cleaning, drag reduction, or other related applications. The coating shows excellent stability to UV radiation, acid/alkali stress, and repetitive bending and kneading, as well as extreme repellency to acidic/alkaline droplets. Moreover, the smart coating can be used as a flexible, high-performance, and multifunctional wearable sensor, which is not only responsive to stretching, bending, and torsion for use in human healthcare and human–machine interface applications, but also superhydrophobic to work under wet and corrosive conditions.

Experimental Section

Ink and Coating Preparation: MWCNTs with an average length of 0.5–2 µm and an average diameter of 10–20 nm (>95 wt% purity) were purchased from Nanjing XFNANO Materials Tech Co., Ltd., China. The TPE was purchased from Gainshine, China. Fe_3O_4 nanopowders of 110 nm were bought from Beisile, China. All materials were used as received. First, MWCNTs (60 mg, with an additional 10 mg of Fe_3O_4 nanopowders for the magnetic ink) were dispersed in cyclohexane (200 mL) by strong sonication (300 W) for 1.5 h using an ultrasonic cell disruptor (BILON 92-II, Shanghai Bilon Co., Ltd., China), and this was followed by the dissolution of the TPE elastomer (60 mg) by magnetic stirring for 10 min and another 1.5 h of sonication (300 W) to form a suspension (ink). In the following experiments, the as-prepared ink was coated onto various substrates, including glass, PET, cloth, and copper, to form thin layers of MWCNT/TPE (or magnetic MWCNT/Fe_3O_4/TPE) films using a spray-gun. The air pressure for spraying was maintained at 45 psi, the distance between the spray-gun and the substrates was ≈10 cm, and the spraying speed was ≈0.5 cm s^{-1}. Thereafter, the coated substrates were immersed in absolute ethanol for ≈2 min and dried in air for at least 5 min before testing.

Sensor Preparation: Strips of CNT/TPE-film sensors with a size of 30 mm × 30 mm × 1 µm ($L_0 \times W_0 \times t_0$) were coated on silicone rubber (Dow Corning Sylgard 184) substrates using paper masks. The silicone rubber substrates were obtained by pouring a premix of silicone monomer and a curing agent in a 1:1 weight ratio into homemade molds and curing at 80 °C.

Characterization: A digital camera (Canon EOS 70D) was used to take the optical photographs and videos in this study. Scanning electron microscopy was performed to observe the micromorphology with a Hitachi S-4800 cold field emission SEM at an accelerating voltage of 5 kV. AFM measurement was performed to characterize the surface height variation on a Veeco Dimension-ICON instrument in noncontact mode. A stepper machine (BeiJing Optical Century Instrument Co., Ltd., China) was used to stretch the coated CNT/TPE sensor on a piece of silicone rubber with one end fixed and the other end linearly elongated at constant speed. Resistance measurements were carried out by connecting the two ends of the CNT/TPE-film sensor to a digital source meter (Keithley 2602A), with conductive copper wires to record the real-time electric current (I) flowing through the film under a constant voltage (V_0) of 4 V, while the real-time resistance (R) was calculated by the equation $R = V_0 / I$.

Supporting Information

Supporting Information is available from the Wiley Online Library or from the author.

Acknowledgements

L.H.L. and Y.Y.B. contributed equally to this work. This work was supported by the National Natural Science Foundation of China (61574163), the Science Foundation for Distinguished Young Scholars of Jiangsu Province, China (BK20170008) and the CAS Key Laboratory of Nano-Bio Interface, Suzhou Institute of Nano-Tech and Nano-Bionics, Chinese Academy of Sciences. The NANO-X Workstation scientifically supported this research. This infrastructure would not be possible without the significant contributions of the Chinese Academy of Sciences, Suzhou Industrial Park, Suzhou City, Jiangsu Province. The human subject involved in the experiments took part with informed consent.

Conflict of Interest

The authors declare no conflict of interest.

Keywords

carbon nanotubes, flexible sensors, multifunction, superhydrophobicity, wearable electronics

Received: May 5, 2017
Revised: July 25, 2017
Published online: September 22, 2017

[1] a) L. Feng, S. H. Li, Y. S. Li, H. J. Li, L. J. Zhang, J. Zhai, Y. L. Song, B. Q. Liu, L. Jiang, D. B. Zhu, *Adv. Mater.* **2002**, *14*, 1857; b) W. Barthlott, C. Neinhuis, *Planta* **1997**, *202*, 1.
[2] R. Blossey, *Nat. Mater.* **2003**, *2*, 301.
[3] a) D. L. Hu, B. Chan, J. W. M. Bush, *Nature* **2003**, *424*, 663; b) X. F. Gao, L. Jiang, *Nature* **2004**, *432*, 36.
[4] X. C. Tian, S. Shaw, K. R. Lind, L. Cademartiri, *Adv. Mater.* **2016**, *28*, 3677.
[5] Y. Lu, S. Sathasivam, J. L. Song, C. R. Crick, C. J. Carmalt, I. P. Parkin, *Science* **2015**, *347*, 1132.

[6] a) W. Barthlott, T. Schimmel, S. Wiersch, K. Koch, M. Brede, M. Barczewski, S. Walheim, A. Weis, A. Kaltenmaier, A. Leder, H. F. Bohn, *Adv. Mater.* **2010**, *22*, 2325; b) F. Feuillebois, M. Z. Bazant, O. I. Vinogradova, *Phys. Rev. Lett.* **2009**, *102*, 026001.
[7] a) C. Cottin-Bizonne, J. L. Barrat, L. Bocquet, E. Charlaix, *Nat. Mater.* **2003**, *2*, 237; b) P. Joseph, C. Cottin-Bizonne, J. M. Benoit, C. Ybert, C. Journet, P. Tabeling, L. Bocquet, *Phys. Rev. Lett.* **2006**, *97*, 156104.
[8] J. K. Yuan, X. G. Liu, O. Akbulut, J. Q. Hu, S. L. Suib, J. Kong, F. Stellacci, *Nat. Nanotechnol.* **2008**, *3*, 332.
[9] X. J. Feng, L. Jiang, *Adv. Mater.* **2006**, *18*, 3063.
[10] J. F. Zang, S. Ryu, N. Pugno, Q. M. Wang, Q. Tu, M. J. Buehler, X. H. Zhao, *Nat. Mater.* **2013**, *12*, 321.
[11] D. Oner, T. J. McCarthy, *Langmuir* **2000**, *16*, 7777.
[12] J. Genzer, K. Efimenko, *Science* **2000**, *290*, 2130.
[13] K. K. S. Lau, J. Bico, K. B. K. Teo, M. Chhowalla, G. A. J. Amaratunga, W. I. Milne, G. H. McKinley, K. K. Gleason, *Nano Lett.* **2003**, *3*, 1701.
[14] H. Y. Erbil, A. L. Demirel, Y. Avci, O. Mert, *Science* **2003**, *299*, 1377.
[15] G. R. J. Artus, S. Jung, J. Zimmermann, H. P. Gautschi, K. Marquardt, S. Seeger, *Adv. Mater.* **2006**, *18*, 2758.
[16] X. Deng, L. Mammen, H. J. Butt, D. Vollmer, *Science* **2012**, *335*, 67.
[17] a) J. H. Zou, H. Chen, A. Chunder, Y. X. Yu, Q. Huo, L. Zhai, *Adv. Mater.* **2008**, *20*, 3337; b) J. E. Mates, I. S. Bayer, J. M. Palumbo, P. J. Carroll, C. M. Megaridis, *Nat. Commun.* **2015**, *6*, 8874; c) N. R. Chiou, C. M. Lui, J. J. Guan, L. J. Lee, A. J. Epstein, *Nat. Nanotechnol.* **2007**, *2*, 354; d) Y. Zhu, J. C. Zhang, Y. M. Zheng, Z. B. Huang, L. Feng, L. Jiang, *Adv. Funct. Mater.* **2006**, *16*, 568.
[18] Z. B. Huang, Y. Zhu, J. H. Zhang, G. F. Yin, *J. Phys. Chem. C* **2007**, *111*, 6821.
[19] a) R. H. Baughman, A. A. Zakhidov, W. A. de Heer, *Science* **2002**, *297*, 787; b) L. B. Zhu, J. W. Xu, Y. H. Xiu, Y. Y. Sun, D. W. Hess, C. P. Wong, *Carbon* **2006**, *44*, 253.
[20] R. N. Wenzel, *Ind. Eng. Chem.* **1936**, *28*, 988.
[21] C. Peinado, T. Corrales, F. Catalina, S. Pedron, V. R. S. Quiteria, M. D. Parellada, J. A. Barrio, D. Olmos, J. Gonzalez-Benito, *Polym. Degrad. Stab.* **2010**, *95*, 975.
[22] T. Q. Trung, N. E. Lee, *Adv. Mater.* **2016**, *28*, 4338.
[23] a) C. Y. Wang, X. Li, E. L. Gao, M. Q. Jian, K. L. Xia, Q. Wang, Z. P. Xu, T. L. Ren, Y. Y. Zhang, *Adv. Mater.* **2016**, *28*, 6640; b) Y. Cheng, R. R. Wang, J. Sun, L. Gao, *Adv. Mater.* **2015**, *27*, 7365; c) X. Q. Liao, Q. L. Liao, X. Q. Yan, Q. J. Liang, H. N. Si, M. H. Li, H. L. Wu, S. Y. Cao, Y. Zhang, *Adv. Funct. Mater.* **2015**, *25*, 2395; d) S. Harada, W. Honda, T. Arie, S. Akita, K. Takei, *ACS Nano* **2014**, *8*, 3921.
[24] a) Y. Li, S. D. Luo, M. C. Yang, R. Liang, C. C. Zeng, *Adv. Funct. Mater.* **2016**, *26*, 2900; b) B. U. Hwang, J. H. Lee, T. Q. Trung, E. Roh, D. I. Kim, S. W. Kim, N. E. Lee, *ACS Nano* **2015**, *9*, 8801; c) J. T. Muth, D. M. Vogt, R. L. Truby, Y. Menguc, D. B. Kolesky, R. J. Wood, J. A. Lewis, *Adv. Mater.* **2014**, *26*, 6307; d) N. S. Lu, C. Lu, S. X. Yang, J. Rogers, *Adv. Funct. Mater.* **2012**, *22*, 4044; e) D. J. Lipomi, M. Vosgueritchian, B. C. K. Tee, S. L. Hellstrom, J. A. Lee, C. H. Fox, Z. N. Bao, *Nat. Nanotechnol.* **2011**, *6*, 788.
[25] E. Roh, B. U. Hwang, D. Kim, B. Y. Kim, N. E. Lee, *ACS Nano* **2015**, *9*, 6252.
[26] a) T. Yamada, Y. Hayamizu, Y. Yamamoto, Y. Yomogida, A. Izadi-Najafabadi, D. N. Futaba, K. Hata, *Nat. Nanotechnol.* **2011**, *6*, 296; b) J. Kim, M. Lee, H. J. Shim, R. Ghaffari, H. R. Cho, D. Son, Y. H. Jung, M. Soh, C. Choi, S. Jung, K. Chu, D. Jeon, S. T. Lee, J. H. Kim, S. H. Choi, T. Hyeon, D. H. Kim, *Nat. Commun.* **2014**, *5*, 5747.
[27] C. Y. Yan, J. X. Wang, W. B. Kang, M. Q. Cui, X. Wang, C. Y. Foo, K. J. Chee, P. S. Lee, *Adv. Mater.* **2014**, *26*, 2022.